



## SYNTHESIS, CHARACTERIZATION AND GAS SENSING PERFORMANCE OF SOL-GEL PREPARED NANOCRYSTALLINE SnO<sub>2</sub> THIN FILMS

Ramesh H. Bari<sup>1\*</sup>, Sharad.B. Patil<sup>1</sup>, Anil.R. Bari<sup>2</sup>

<sup>1\*</sup> Nanomaterials Research Laboratory, Department of Physics, G. D. M. Arts, K. R. N. Commerce and M.D. Science College, Jamner 424 206, India.

<sup>2</sup> Department of Physics, Arts, Commerce and Science College, Bodwad 425 310, India.

\*Corresponding author: [rameshbari24@yahoo.com](mailto:rameshbari24@yahoo.com)

---

**Submitted: Nov. 15, 2013**

**Accepted: Apr. 21, 2014**

**Published: June 1, 2014**

---

**Abstract** - *Nanocrystalline SnO<sub>2</sub> thin films were successfully prepared using sol-gel dip coating technique. The starting precursor was used as tin chloride dihydrate (SnCl<sub>2</sub>·2H<sub>2</sub>O), ethanol and glycerin. As the prepared films were fired at 500°C. These films were characterized using XRD, FE-SEM and TEM to known crystal structure, surface morphology and microstructure property. Elemental composition was studied using energy dispersive spectrophotometer (EDAX). The H<sub>2</sub> gas sensing performance of nanocrystalline SnO<sub>2</sub> thin films were investigated and presented. It was found that the nanocrystalline SnO<sub>2</sub> thin films gives maximum gas response (S= 360) at 75 °C. The sensor shows fast speed of response (T<sub>Response</sub> = 2 s) and quick recover (T<sub>recover</sub> = 8 s).*

**Index terms:** Sol-gel, nanocrystalline SnO<sub>2</sub>, thin films, H<sub>2</sub> gas sensor, fast response-recovery.

---

## I. INTRODUCTION

In recent years, semiconductor metal oxide have received considerable attention because of their possible application in gas sensor, solar cells, photochemical and photoconductive device, liquid crystal display, gas discharge display, lithium-ion batteries, etc.[1-3]. SnO<sub>2</sub> is an n- type semiconductor which has a strong gas sensing properties. In particular, the size of crystalline forming the gas response layer determines both the absolute gas sensitivity and the signal stability. In order to achieve the maximum gas response the grain size must be smaller than two times of depleting layer [4].

In general, the semiconductor metal oxide gas sensor like SnO<sub>2</sub>, ZnO, WO<sub>3</sub> [5-7] have been widely studies due to their range of conducting variability and their response towards both the oxidizing and reducing gases. They are used in the form of bulk material. Thick or thin films gas sensing is basically the surface phenomenon and hence thin films sensor have advantage due to their higher surface to volume ratio [8].

Hydrogen can be mainly used for energy generations in the near future due to the fact that fuel cell electricity generators are clean, quiet and more efficient than any other known technology. It is therefore straightforward that in all these applications safety measures are of highest concern due to the explosive properties of hydrogen [4].

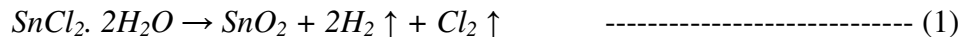
A variety of techniques have been used to prepare tin oxide (SnO<sub>2</sub>) thin films. These include spray pyrolysis [9], chemical vapour deposition [10], activated reactive evaporation [11], ion-beam assisted deposition [12] and sputtering [13] among these techniques sol-gel dip coating technique has proved to be simple, reproducible and inexpensive, as well as suitable for large area applications. However it is only for last one or two decades that considerable interest, both in scientific and industrial fields, has been generated due to the realization of the several advantages one gets as compared to some other techniques. Sol-gel dip coating formation is usually a low temperature process; it requires less energy consumption and causes less pollution too. In the present study the synthesis of nanostructured SnO<sub>2</sub> thin films for structural, microstructure analysis and H<sub>2</sub> gas sensor at low operating temperature (75 °C) were studied.

## II. EXPERIMENTAL DETAILS

### a. Preparation of nanocrystalline SnO<sub>2</sub> thin films

Firstly, 0.1M Tin (II) chloride dihydrate (SnCl<sub>2</sub>.2H<sub>2</sub>O), Purified Merck) was dissolved in ethanol. The solution was stirred by a magnetic stirring apparatus for 30 minute. After that the sol was mixed with glycerin as a dispersion stabilizer at volume ratio of 15:1 to obtain the sol-gel for dip coating.

Glass substrate was immersed into the solution for 10 sec. draw vertically, laid flatly and then wet thin films formed. Thus the films with different dipping time cycle of 5, 10 and 15 were obtained and referred as sample S1, S2 and S3 respectively. Finally the thin films were annealed at temperature 500 °C for 1 hrs. SnO<sub>2</sub> formulation can be represented as:



### b. Sensing system to test the gases

Figure 1 shows block diagram of gas sensing system. The gas sensing studies were carried out using a static gas chamber to sense H<sub>2</sub> gas in air ambient. The nanostructured SnO<sub>2</sub> thin films were used as the sensing elements. Cr-Al thermocouple is mounted to measure the temperature. The output of thermocouple is connected to temperature indicator. Gas inlet valve fitted at one of the ports of the base plate. Gas concentration (500 ppm) inside the static system is achieved by injecting a known volume of test gas in gas injecting syringe. Voltage is applied to the sensor and current can be measured by picoammeter.

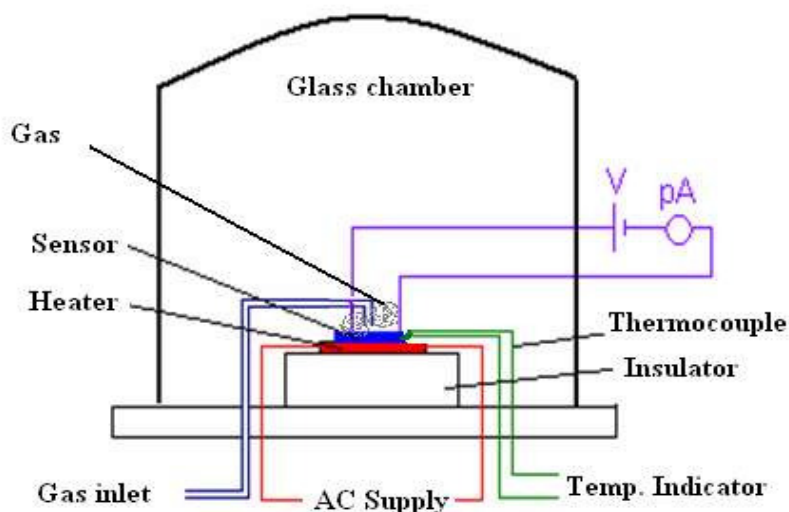


Figure 1. Block diagram of gas sensing system

### III. MATERIAL CHARACTERIZATIONS

The nanostructured SnO<sub>2</sub> thin films were characterized by X-ray diffraction ((Miniflex Model, Rigaku, Japan), using CuK $\alpha$  radiation with a wavelength,  $\lambda = 1.5418 \text{ \AA}$ ). The microstructure of the films was analyzed using a field emission scanning electron microscope (FE-SEM, JEOL. JED 6300) and Transmission electron microscope (TECNAI G<sup>2</sup> 20 - TWIN (FET, NETHERLAND). Element composition of the films was analyzed energy dispersive spectrophotometer (JEOL 2300 model, Japan) and Electrical and gas sensing properties were measured using a static gas sensing system. The sensor performance on exposure of liquefied petroleum gas (LPG), carbon dioxide (CO<sub>2</sub>), carbon monoxide (CO), hydrogen (H<sub>2</sub>), ammonia (NH<sub>3</sub>), ethanol (C<sub>2</sub>H<sub>5</sub>OH), chlorine (Cl<sub>2</sub>) and Hydrogen sulfide (H<sub>2</sub>S) was examined.

## a.X-ray diffraction analysis

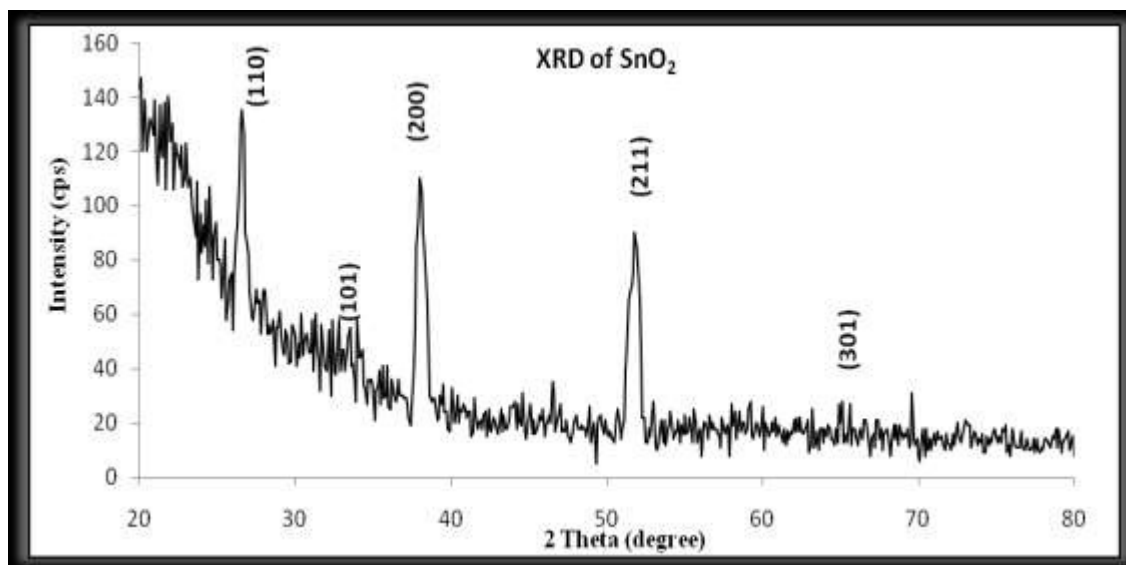


Figure 2. X-ray diffractogram of most sensitive nanocrystalline SnO<sub>2</sub> thin film (Sample =S2)

Figure 2 shows the X-ray diffractogram of most sensitive nanostructured SnO<sub>2</sub> thin film (Sample = S2). Diffraction pattern was obtained with  $2\theta$  from  $20^\circ$  to  $80^\circ$ . The XRD pattern of the film shows that as the synthesized film is polycrystalline in structure and nanocrystalline in nature, with the tetragonal phase and shows preferential orientation along c-axis. The result is in agreement with the reported ASTM data of pure SnO<sub>2</sub>. The strongest peak observed at  $2\theta = 37.96^\circ$  can be attributed to the (200) plane. The (110), (101), (211) and (301) peaks also observed at  $2\theta = 26.61^\circ$ ,  $33.88^\circ$ ,  $51.75^\circ$ , and  $65.94^\circ$  respectively. The average grain size of nanostructured SnO<sub>2</sub> thin film were calculated by using the Scherrer formula it was given in table 1.

$$D = 0.9\lambda / \Delta(2\theta) \cos\theta \text{ -----(2)}$$

Where,  $D$  = Average crystallite size

$\lambda$  = X-ray wavelength ( $1.542 \text{ \AA}$ )

$\theta$  and  $\Delta(2\theta)$  = Bragg diffraction angle of the XRD peak in degree and the full width at half maximum (in radian) of diffraction peak respectively.

Table1. Measurement grain size from XRD

Reported $2\theta$	Observed $2\theta$	hkl plane	Grain size (nm)
26.57	26.61	110	13.8
33.87	33.88	101	14.2
37.94	37.96	200	14.8
51.74	51.75	211	13.2
65.96	65.94	301	14
Average grain size			14

Grain size was also determined using Williamson – Hall technique [14], by plotting the graph using equation (3).

$$\beta \cos\theta/\lambda = 1/D + \varepsilon (\sin\theta/\lambda) \text{ -----(3)}$$

Where,  $\beta$  = full width at half maxima of peak measured in radian

$\theta$  = diffraction angle

$\lambda$  = wavelength of X-ray

D = grain size

$\varepsilon$  = microstrain

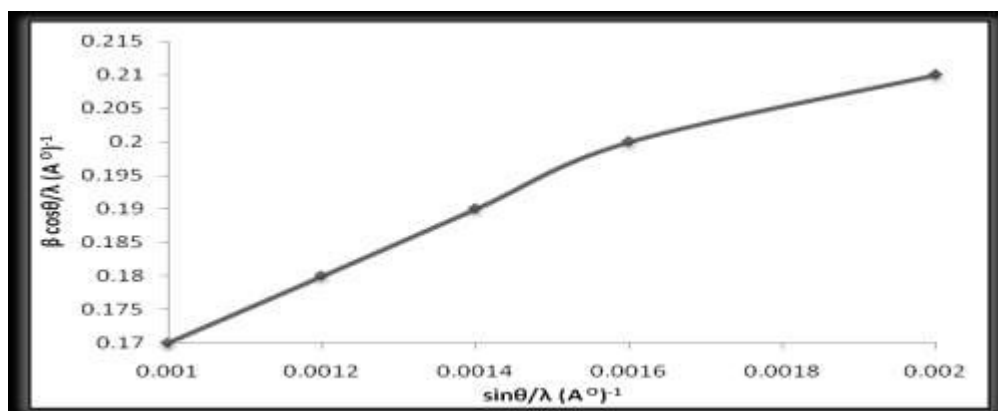


Figure 3. Variation of  $\beta \cos\theta/\lambda$  with  $\sin\theta/\lambda$

Figure 3 represents the plot of  $\beta \cos\theta/\lambda$  and  $\sin\theta/\lambda$  for thin films. The intercept of line on y- axis gives the grain size. It was observed to be 14 nm.

### b. Surface Morphology

The microstructure of the prepared film was analyzed using a field emission scanning electron microscope.

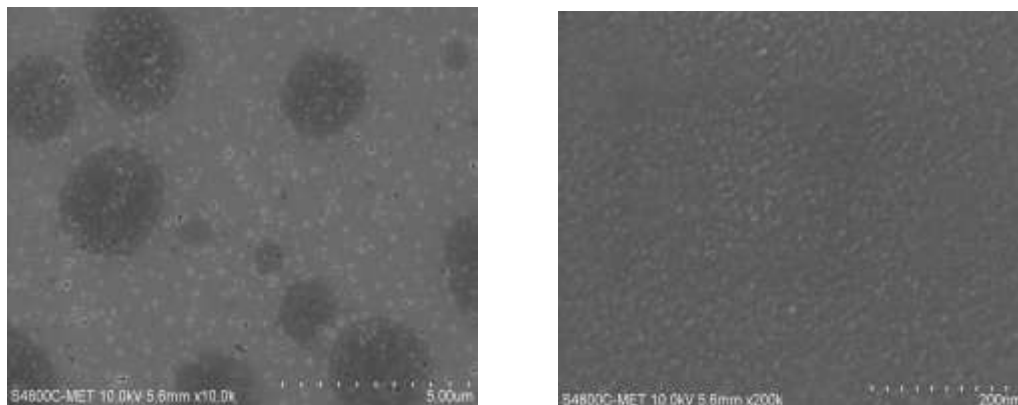


Figure 4. FE-SEM images of most sensitive nanocrystalline SnO<sub>2</sub> thin film sample: (a) Low magnification and (b) High magnification.

The morphology of the particles was uniform distribution and roughly spherical in shape. The average grain size was about 12 nm. Larger particles may be due to the agglomeration of smaller crystallites as shown in the low magnification image as shown in Fig. 4(a). Fig. 4(b) shows the high magnification image, indicating the spherical shape grains.

### c. Transmission electron microscope (TEM)

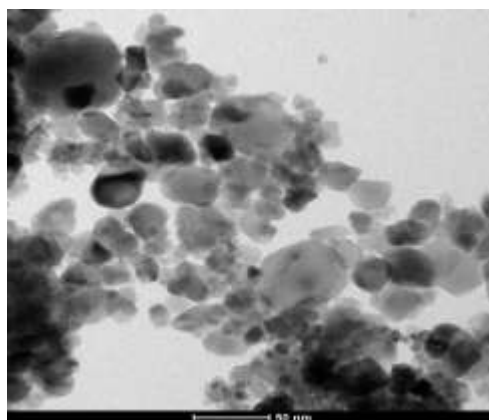


Figure 5. TEM images of most sensitive nanocrystalline SnO<sub>2</sub> thin film: samples S2

Figure 5 shows the TEM of most sensitive nanocrystalline SnO<sub>2</sub> thin films (Sample= S2) obtained by scratching the thin film. The powder was dispersed in ethanol. Copper grid was used

to hold the powder. It is clear from TEM image that the grains are nanocrystalline in nature which are smaller than 9 nm with nearly spherical in shape.

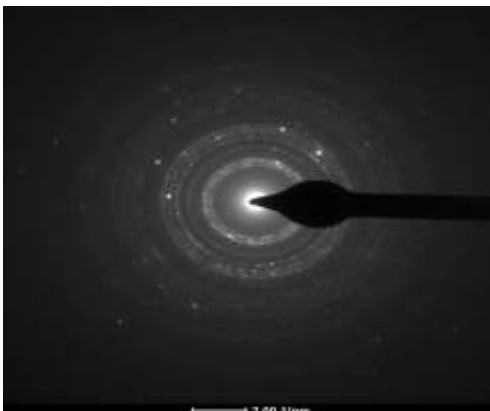


Figure 6. Electron diffraction pattern of nanocrystalline SnO<sub>2</sub> thin film: sample S2.

The electron diffraction pattern of the most sensitive nanostructured SnO<sub>2</sub> thin film sample S2 is shown in Figure 6. It indicates spotty but continuous ring patterns without any additional diffraction spots and rings of secondary phases, revealing their highly crystalline structure.

#### d. Quantitative elemental analysis (EDAX)

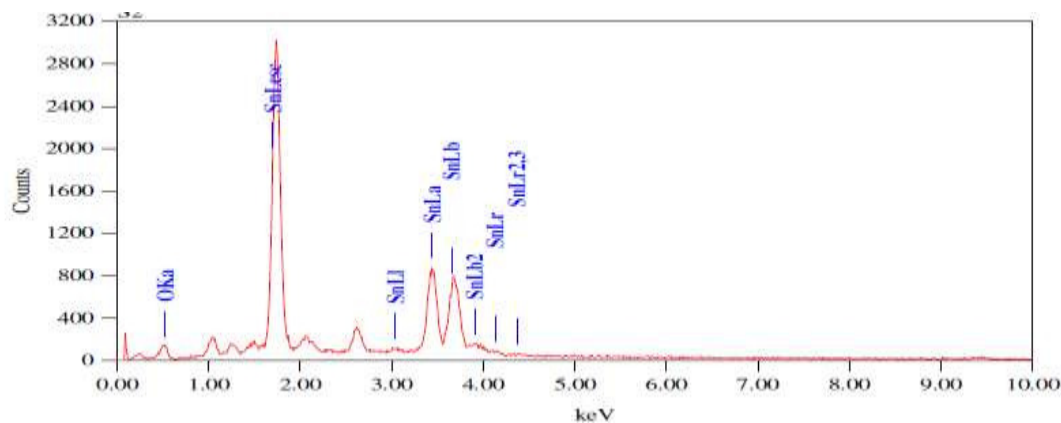


Figure 7. Element analysis of most sensitive nanostructured SnO<sub>2</sub> thin film: sample S2

The quantitative elemental composition of the most sensitive nanocrystalline SnO<sub>2</sub> thin film sample (S2) was analyzed using an energy dispersive spectrometer

Table 2. Quantative elemental analysis as prepared polycrystalline SnO<sub>2</sub> thin film

Element	Observed	
	mass %	at %
O	25.03	71.24
Sn	74.97	28.76
Total	100	100

Stoichiometrically expected at % of Sn and O is: 33.30 and 66.70, respectively, observed at% Of Sn and O (Table 2) were: 28.76 and 71.24, respectively. It is clear from table that as prepared polycrystalline SnO<sub>2</sub> thin film was observed to nonstoichiometric in nature.

#### e. Determination of film thickness

The film thickness was measured by a weight difference method [15] in which weight of the sample, area and densities were considered. In order to measure the thickness of the thin films by using weight difference method, error and accuracy was found to be  $\pm 5$  % nm. The thickness, sample weight and sample area are related as:

$$t = M/A.\rho \text{ ----- (4)}$$

Where,  $M$  is the weight of the sample in gm,

$A$  the area of the sample in cm<sup>2</sup>

and  $\rho$  the materials density in gm cm<sup>-3</sup>.

The thickness of the film was in the range of 105-119 nm. The values of the film thickness with dipping cycle are given in Table 3.

Table 3. Measurement of dipping cycle and film thickness

Sample	Dipping cycle	Thickness (nm)
S1	5	105
S2	10	113
S3	15	119

#### IV. ELECTRICAL PROPETIES

##### a. I–V characteristics

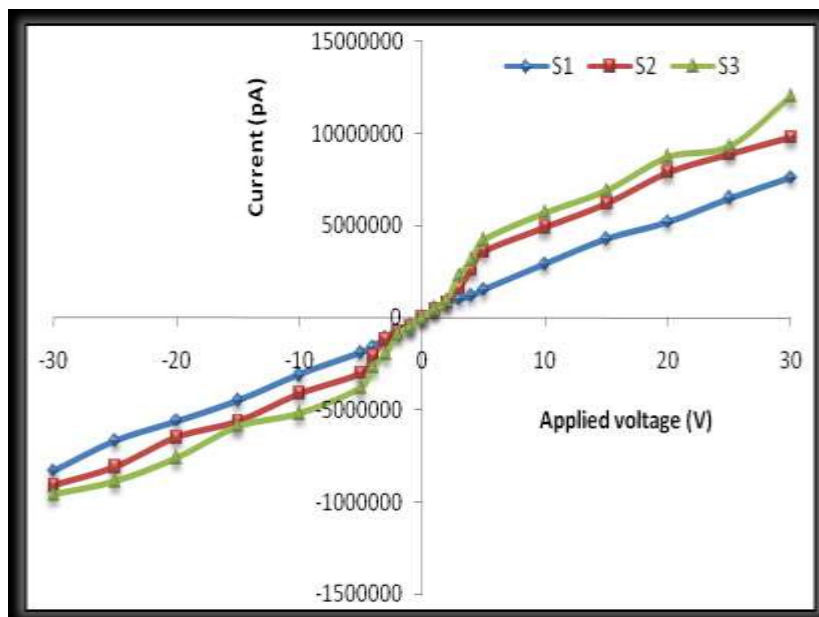


Figure 8. I–V characteristics of nanocrystalline SnO<sub>2</sub> thin film sensors.

The sensor structures were prepared in dimension as: 1.5 cm × 1 cm. The contacts were made by silver paste on thin film surface. Figure 8 shows the I–V characteristics of samples S1, S2, and S3 observed to be nearly symmetrical in nature indicating ohmic contacts. The non-linear I–V characteristics may be due to semiconducting nature of the films. Sample S1, S2, and S3 are the films obtained by dipping cycle intervals of: 5, 10 and 15 respectively. Therefore, the thickness of the films goes on increasing from S1 through S3.

##### b. Electrical conductivity

Figure 9 show the variation of  $\log(\sigma)$  with operating temperature. The conductivity of each sample is observed to be increasing with an increase in temperature range between 50 °C and 150 °C in steps of 25 °C. The increase in conductivity with increase in temperature could be attributed to negative temperature coefficient of resistance and semiconducting nature of nanostructured SnO<sub>2</sub>.

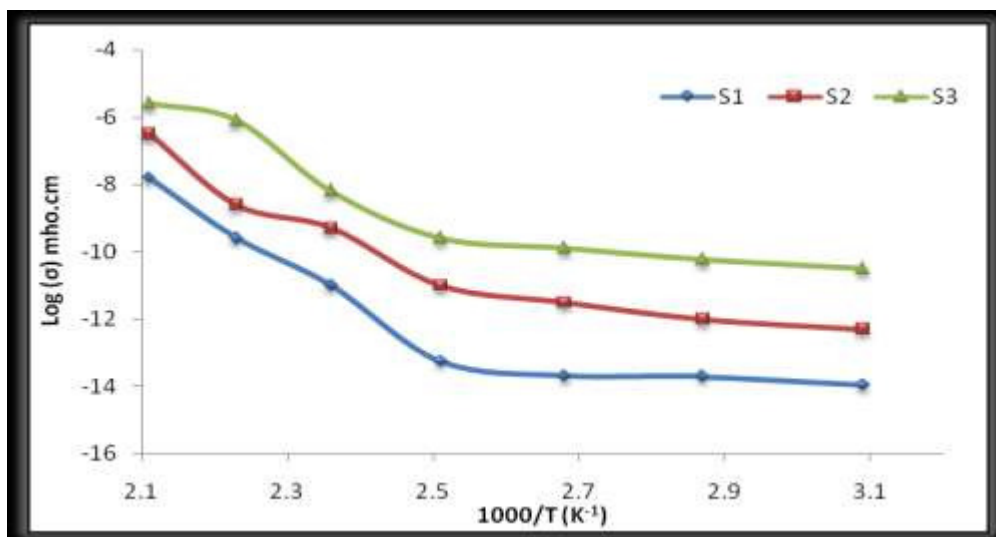


Figure 9. Variation of  $\log(\sigma)$  with operating temperature ( $^{\circ}\text{C}$ ).

For the metal oxide semiconductor thin films it is reported that [16, 17], when thickness of the film increases activation energy goes on decreases. The activation energy calculated from slopes of line for sample S1, S2 and S3 were given in table 4.

Table 4. Measurement of activation energy and film thickness

Sample no.	Thickness (nm)	Activation energy ( $\Delta E$ )	
		30 $^{\circ}\text{C}$	150 $^{\circ}\text{C}$
S1	105	0.50 eV	0.65 eV
S2	113	0.36 eV	0.45 eV
S3	119	0.27 eV	0.32 eV

It is clear from Table 4 that, as film thickness of the sample goes on increasing; while the activation energy goes on decreasing. The decrease in activation energy with increasing film thickness may be due to the change in structural parameters, improvement in crystallite and grain size [18].

### V.GAS SENSING PERFORMANCE OF THE SENSORS

a. Measurement of gas response

Gas response (S) of the sensor is defined as the ratio of change in conductance to the conductance of the sensor on exposure of target (at same operating conditions).

$$S = \frac{G_g - G_a}{G_a} \text{ ----- (5)}$$

Where, G<sub>a</sub> = the conductance of the sensor in air

G<sub>g</sub> = the conductance on exposure of a target gas.

b. Gas response

Figure 10 shows the variation in response with the operating temperature to 500 ppm of H<sub>2</sub> for S1, S2, and S3 samples. For all the samples the response increases with increase in operating temperature and reach maximum (S=360 for sample S2) at 75°C. Response of sensors depends on two factors, namely: the speed of chemical reaction on the surface of the grains, and the speed of the diffusion of gas molecules to that surface. At low temperatures the sensor response is restricted by the speed of chemical reactions. At higher temperature the sensor response is restricted by the speed of the diffusion of gas molecules to that surface. At some intermediate temperature the speed values of two processes become equal, and at that point the sensor response reaches its maximum. According to this mechanism for every gas there is a specific temperature at which the sensor response attains its peak value.

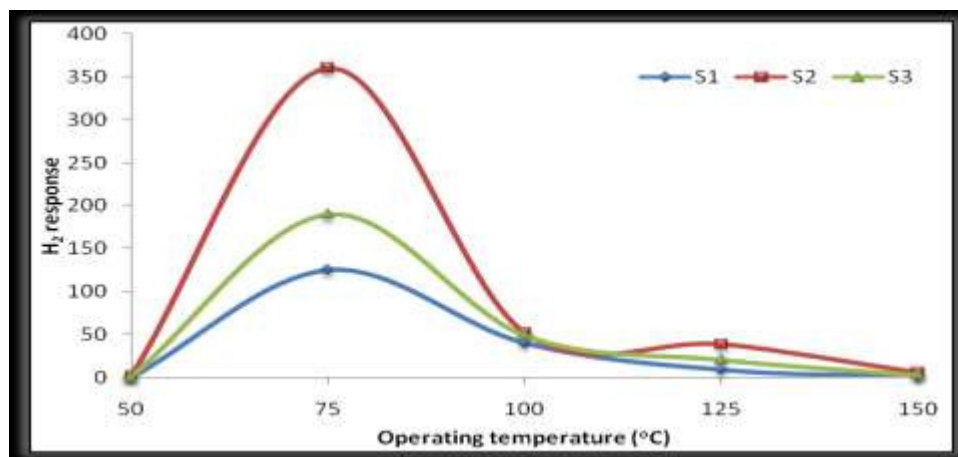


Figure 10. Gas response of pure nanostructured SnO<sub>2</sub> thin films with operating temperature.

### c. Selectivity

Selectivity can be defined as the ability of a sensor to respond to a certain gas in the presence of different gases. Fig 11 shows the histogram for comparison of the H<sub>2</sub> response to various gases for sample S1, S2, S3 at the optimum operating temperature 75 °C and operating voltage (10 V).

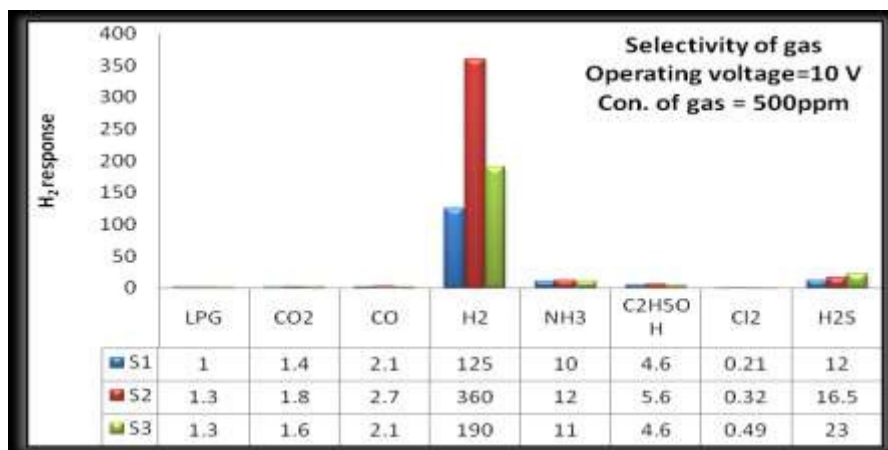


Figure 11. Selectivity of nanocrystalline SnO<sub>2</sub> thin films for different gases.

The table attached to histogram (Fig. 11) shows the gas response values, it is clear that the S2 film is highly selective to H<sub>2</sub> (500 ppm) against all other tested gases: LPG, CO<sub>2</sub>, CO, NH<sub>3</sub>, C<sub>2</sub>H<sub>5</sub>OH, Cl<sub>2</sub> and H<sub>2</sub>S

### d) Response and recovery of the sensor

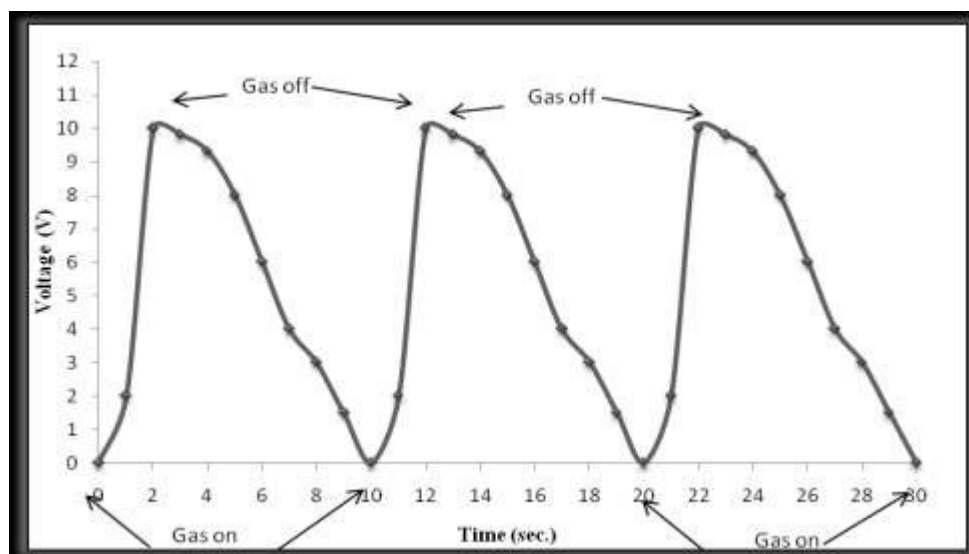


Figure 12. Response and recovery of the sensor (Sample=S2).

The time taken for the sensor to attain 90% of the maximum decrease in resistance on exposure to the target gas is the response time. The time taken for the sensor to get back 90% of original resistance is the recovery time.

The response and recovery of the polycrystalline SnO<sub>2</sub> thin film (S2) sensor on exposure of 500 ppm of H<sub>2</sub> at 75 °C are represented in Fig. 12. The response is quick (2 s) and recovery is fast (8 s). The high oxidizing ability of adsorbed oxygen species on the surface nanoparticles and high volatility of desorbed by-products explain the quick response to H<sub>2</sub> and fast recovery

**Table 5.** Comparison of H<sub>2</sub> response of reported sensors with sensor prepared in the present work

<b>Form of sensor</b>	<b>Concentration (ppm)</b>	<b>Gas response</b>	<b>Operating temperature (° C)</b>	<b>Reference</b>
SnO <sub>2</sub> (Thin)	500	360	75	(Present work) Sample S2
SnO <sub>2</sub> (Thin)	100	13	30	19
TiO <sub>2</sub> (Thin)	1000	8	30	20
ZnO (Thin)	1000	5.9	30	21
Au or Pt enhanced SnO <sub>2</sub> (Thin)	1000-5000	2	150	22
Al -doped	1000	10	100	23
Nb <sub>2</sub> O <sub>5</sub> NW (Thin)	2000	50	20	24

Table 5 presents comparison of H<sub>2</sub> response with reported different sensor and sensor prepared in present investigation.

## VI.DISCUSSION

## a. Gas sensing mechanism

Figure 13 shows the  $H_2$  sensing mechanism (Fig. (a) Before exposure of  $H_2$  and (b) after exposure of  $H_2$ ) of  $SnO_2$  thin films. When the oxidation reaction rate of  $H_2$  is much higher than the rates of adsorption and desorption of the reactants, the steady state oxygen coverage depends critically on the relative oxygen and  $H_2$  concentrations in the gas phase [19, 25]. Oxidation of  $H_2$  on a tin oxide surface may occur through many different reaction paths, depending on the surface composition, structure and temperature and on adsorbed species. Most of the time, the intermediates and complexes formed during reaction are short-living compounds that are not easily identified. However, in order to understand the overall sensing mechanism of  $H_2$ , it is necessary to know what oxygen species are present on the surface and their extent, how does  $H_2$  adsorb on the surface, which reaction paths are possible and which is the rate of each step, what other elements may interfere in the reaction and if they are present.

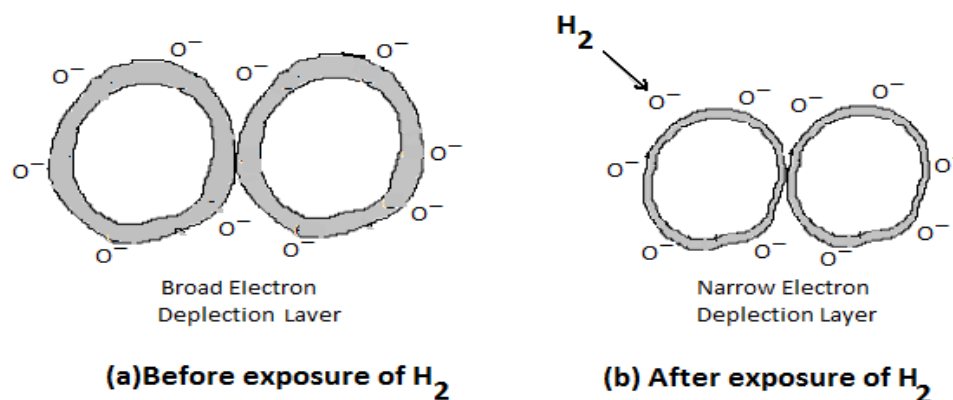


Figure 13. Sensing mechanism of  $SnO_2$  thin film

The response of the sensing materials is based on chemisorption, i.e. the exchange of charge between absorbed gases and the metal oxide surface [24, 25]. In air, there are several different negatively charged oxygen adsorbates, such as O<sub>2</sub><sup>-</sup>, O<sup>-</sup>, and O<sup>2-</sup>, which are known to cover the metal oxide surface. The formation of an oxygen adsorbate layer leads to a decrease in the electron density on the metal oxide surface due to charge transfer from the metal oxide to the adsorbate layer. When the metal oxide used as a sensing material is exposed to reducing gas molecules, the gas molecules are oxidized by the oxygen ions on the metal oxide surface, resulting in the release of free electrons to the metal oxide and consequently, to an increase in the conductance (decrease of resistance) of the metal oxide [25]. This implies that the gas sensing behavior of a metal oxide semiconductor is strongly related to its surface properties. Then, by varying the surface morphology, it is possible to tune the gas sensing properties of a material. Indeed, depending on surface properties of the nanocrystallites, a unique combination of structural, electronic, and adsorption/desorption process parameters can be obtained, thus the design of nanomaterials with controlled shape and/or morphology can participate to the enhancement of the sensing properties [4].

When they are operated in the semiconducting temperature range, the overall resistance of the sensor element is determined by the charge transfer process produced by surface reaction and by the transport mechanism from one electrode to the other through sensing layer, Therefore the microstructure of the sensing layer plays a key role for the development of an effective gas sensor [1, 4].

## VII. CONCLUSIONS

Nanocrystalline SnO<sub>2</sub> thin films were prepared by simple and inexpensive sol-gel dip coating technique. Thickness of the films was observed to increase from 105 to 119 nm with increase in dipping time interval. The structural and microstructural properties confirm that the as-prepared SnO<sub>2</sub> thin films are polycrystalline in structure and nanocrystalline in nature. The elemental analysis confirms that so prepared thin films was nonstoichiometric in nature. Nanocrystalline SnO<sub>2</sub> thin film sensor shows a high response to H<sub>2</sub> gas at low operating temperature 75 °C .The sensor showed good selectivity to H<sub>2</sub> gas against LPG, CO<sub>2</sub>, CO, NH<sub>3</sub>, C<sub>2</sub>H<sub>5</sub>OH, Cl<sub>2</sub> and H<sub>2</sub>S gases. The nanocrystalline SnO<sub>2</sub> thin film exhibits rapid response–recovery which is one of the main features of this sensor. The results obtained by sol-gel technique are promising for the preparation of sensitive and low cost hydrogen sensor operating at low temperatures.

## ACKNOWLEDGEMENT

The authors are thankful to the University Grants Commission, New Delhi for providing financial support. Thanks to Principal, G. D. M. Arts, K. R. N. Commerce and M.D. Science College, Jamner, for providing laboratory facilities for this work.

## REFERENCES

- [1] S. B. Deshmukh , R. H. Bari , G. E. Patil , D. D. Kajale , G. H. Jain , L. A. Patil “ Preparation and characterization of zirconia based thick film resistor as a ammonia gas sensor”, *International journal on smart sensing and intelligent systems*, Vol. 5, no. 3, pp.540–558, 2012.

- [2] S. Chappel, A. Zaban, "Nanoporous SnO<sub>2</sub> electrodes for dye-sensitized solar cells: improved cell performance by the synthesis of 18nm SnO<sub>2</sub> colloids", *Solar Energy Materials a Solar Cells*, Vol.71, pp.141–152, 2002.
- [3] S. Gnanam, V. Rajendran, "Luminescence properties of EG- assisted SnO<sub>2</sub> nanoparticles by sol-gel process", *Digest Journal of Nanomaterials and Biostructures*, 5, pp.699-704, 2010.
- [4] L.A. Patil, M.D. Shinde, A.R. Bari, V.V. Deo, "Highly sensitive and quickly responding ultrasonically sprayed nanostructured SnO<sub>2</sub> thin films for hydrogen gas sensing", *Sensors and Actuators B*, Vol.143, pp.270–277, 2009.
- [5] Y. Shimizu, E.D. Bartolomeo, E. Traversa, G. Gusmano, T. Hyodo, K.Wada, M. Egashira, "Effect of surface modification on NO<sub>2</sub> sensing properties of SnO<sub>2</sub> varistor-type sensors", *Sensors and Actuators B*, Vol.60, pp.118–124, 1999.
- [6] R. H. Bari, S.B.Patil, A.R. Bari, G.E.Patil, J. Aambekar, "Spray pyrolysed nanostructured ZnO thin film sensors for ethanol gas", *Sensors & Transducers*, Vol.140, pp.124-132, 2012.
- [7] M. Stankova, X. Vilanova, J. Calderer, I. Gràcia, C. Cané, X. Correig, "Nanograin WO<sub>3</sub> Thin films as active layer for resistive type gas sensors", *Journal of Optoelectronics and Advanced Materials*, Vol. 7, No. 3, pp. 1237 – 1242, 2005.
- [8] S. D. Shinde , G. E. Patil, D. D. Kajale, D. V. Ahire, V. B. Gaikwad and G. H. Jain, "Synthesis of ZnO nanorods by hydrothermal method for gas sensor applications" *International journal on smart sensing and intelligent systems*, Vol. 5, no. 1, pp.57-70, 2012.
- [9] K. Murakami, K. Nakajima, S. Kaneko, "Initial growth of SnO<sub>2</sub> thin film on the glass substrate deposited by the spray pyrolysis technique", *Thin Solid Films*, Vol.515, pp.8632-8636, 2007.
- [10] T. Okuno, T. Oshima, S. Dong Lee, S. Fujita, "Growth of SnO<sub>2</sub> crystalline thin films by mist chemical vapour deposition method", *Physica status solidi (c)*, Vol. 8, 540-542, 2011.
- [11] H.S. Randhawa, M.D. Matthews, R.F. Bunshah, "SnO<sub>2</sub> films prepared by activated reactive evaporation", *Thin Solid Films*, Vol. 83, pp.267-271, 1981.

- [12] T. Mohanty, Y. Batra, A. Tripathi, D. Kanjilal, "Nanocrystalline SnO<sub>2</sub> formation using energetic ion beam", *Journal of Nanoscience Nanotechnology*, Vol. 7, pp.2036-2040, 2007.
- [13] T. Gui, L.Hao, J. Wang, L. Yuan, W. Jai, X. Dong, "Structure and features of SnO<sub>2</sub> thin films prepared by RF reactive sputtering", *Chineses Optics Letters*, Vol. 8, pp.10134-03, 2010.
- [14] S.B. Quadri, E.F. Skelton, D. Hsu, A.D. Dinsmore, J. Yang, H.F. Gray, B.R. Ratna, "Size-induced transition-temperature reduction in nanoparticles of ZnS", *Physical Review B*, Vol. 60, pp.9191–9193, 1999.
- [15] V. B. Patil, G. S. Shahane and L. P. Deshmukh, "Studies on photoelectrochemical (PEC) cells; A correlation between electrochemical and material properties", *Materials Chemistry and Physics*, Vol. 80, pp.625-632, 2003.
- [16] R. H. Bari, S. B. Patil, P. P. Patil, A. R. Bari, "Detection of H<sub>2</sub>S gas at lower operating temperature using sprayed nanostructured In<sub>2</sub>O<sub>3</sub> thin films", *Bulletin of Material Science*, Vol. 36, No. 6, pp. 967–972, 2013.
- [17] R. H. Bari, S. B. Patil, A. R. Bari, "Influence of precursor concentration solution on CO sensing performance of sprayed nanocrystalline SnO<sub>2</sub> thin films", *Optoelectronics and advanced materials rapid communication*, Vol. 6, pp.887-895, 2012.
- [18] R. B. Kale, C. D. Lokhande, "Band gap shift, structural characterization and phase transformation of CdSe thin films from nanocrystalline cubic to nanorod hexagonal on air annealing" *Semiconductor Science Technology*, Vol. 20, pp.1-7, 2005.
- [19] G. E. Patil, D. D. Kajale, D. N. Chavan, N. K. Pawar, V. B. Gayakwad, G. H. Jain, "Spray pyrolysed polycrystalline tin oxide thin films as hydrogen sensor", *Sensors & Transducers*, Vol.12, pp.70-79, 2010.
- [20] C.S.Rout, G.U Kulkarni, C. N. Rao, "Room temperature hydrogen and hydrocarbon sensors based on single nanowires of metal oxides", *Journal of Physics D: Applied Physics*, Vol. 40, pp.2777–2782, 2007.
- [21] Z.H Lim, Z.X Chia, M. Kevin, A. S. W. Wong, G.W. Ho, "A facile approach towards ZnO nanorods conductive textile for room temperature multifunctional sensors", *Sensors and Actuators B*, Vol, 151, pp.121–126, 2010.

- [22] V.E Galstyan, V.M Aroutiounian, V.M Arakelyan, G.E. Shahnazaryan, “Investigation of hydrogen sensor made of ZnO: Al thin film”, *American Journal of Physics*, Vol. 1, pp.242–246, 2009.
- [23] Z.Wang, Y Hu, W Wang,X Zhang,B Wang,H Tian, Y Wang,J.Guan, H.Gu, “Fast and highly-sensitive hydrogen sensing of Nb<sub>2</sub>O<sub>5</sub> nanowires at room temperature”, *Internatinal Journal of Hydrogen Energy* ,Vol.37, pp.4526–4532, 2012.
- [24] C. Xu, J. Tamaki, N. Miura and N. Yamazoe, “Grain size effects on gas sensitivity of porous SnO<sub>2</sub>-based elements”, *Sensors and Actuators*, Vol. 3, pp.147–155, 1991.
- [25] S. D. Shinde, G. E. Patil, D. D. Kajale, V. G. Wagh, V. B. Gaikwad and G. H. Jain, “Effect of annealing on gas sensing performance of nanostructured ZnO thick film resistors”, *International journal on smart sensing and intelligent systems*, Vol. 5, no. 1, pp.277–294, 2012.

\*\*\*\*\*